Multifractal and joint multifractal description of available nutrient concentrations extracted by two methods along short transects

Abstract Spatial variability of available P, K, Ca and Mg, sampled along two short transects and determined with two different extraction methods, was characterized using multifractal and joint multifractal analysis. Sixty six soil samples were collected every 0.8 m, both in a vineyard and in a field with polyculture in rotation. Available nutrients were extracted with an ion exchange resin and the Mehlich 3 solution. Shape and width of singularity, $f(\alpha)$ versus α, and generalized dimension, Dq, spectra, showed that spatial distributions obtained by the two tests behaved as quasi monofractals in the vineyard, but were fitted with multifractal models under polyculture. Joint multifractal analysis demonstrated positive correlations between the scaling indices of P, K, Ca and Mg, extracted by resin and Mehlich 3, which were stronger under polyculture. Pearson correlations between available nutrients determined by two tests at the single scale ranged from $R^2 = 0.54$ to 0.95 and were weaker than those of the respective scaling indices across the range of scales studied, which varied from $R^2 = 0.63$ to 0.97. The joint multifractal approach showed that single scale analysis may be insufficient to compare relationships between available nutrient tests. Moreover, multifractal analysis may be useful to upscaling/downscaling nutrient availability.

Key words: Macronutrients, Soil testing, Spatial variability, Multifractal analysis.

Introduction

Spatial variability of soil physical, chemical and biological properties collected using different sampling strategies and at various scales has been found to be rather a rule than an exception (Mc Bratney and Webster 1986; Zeleke and Si 2006). Both soil forming factors and processes of soil formation and soil use and management strategies account for these variability. In this context, assessing the spatial variability of soil nutrient concentrations is crucial when managing soil fertility and may be useful in refining agricultural practices and improving land use sustainability (Morales et al. 2011; Zhang et al. 2013).

Patterns of variability and heterogeneity of soil properties have been successfully quantified since the 1980s from spatially-sampled point measurements, using geostatistical techniques (Mc Bratney and Webster 1986; Caridad Cancela et al. 2005; Morales et al. 2011). However, the geostatistical approach, which is based on a second-order moment, the semivariogram, has been not always able to address how a variable changes with scale or frequency, especially in the presence of singularities. This is because geostatistics is subjected to the assumption of stationarity, meaning a semivariogram can only provide a poor characterization of the variability that occurs in a body of data with non-normal distributions (Zeleke and Si 2006; Bertol et al. 2017). In other words, spatially sampled data sets with singularities usually are non-stationary, cannot be described by a normal distribution, and subsequently their complete characterization demand higher moments orders than the second moment employed in geostatistical studies (Caniego et al. 2005; Zeleke and Si 2006; Zhang et al. 2013; Vidal-Vázquez et al. 2013).

Scaling analysis, such as fractal analysis (Armstrong 1986; Perfect and Kay 1995, Vidal Vázquez et al. 2006) and multifractal analysis (Grout et al. 1998; Miranda et al.

2006; Ji et al. 2016), has been also used to adequately characterize the spatial variability of soil properties. The fractal approach is considered to be only valid when the spatial distribution of the studied variable is the response of some (one or a few) linear processes. Most frequently, however, and following the seminal work of Everstz and Mandelbrot (1992), the spatial distribution of soil properties has been identified as a nonlinear response, because heterogeneity and variability are driven by multiple factors and processes operating at different intensities and over a variety of scales (Caniego et al. 2005; Vidal Vázquez et al. 2013; Zhang et al. 2013). Therefore, since the end of 1990s, multifractal analysis, has been used to quantify several soil properties (Grout et al. 1998; Roisin et al. 2007; Vidal Vázquez et al. 2008; Paz-Ferreiro et al. 2010), and also the spatial variability of soil properties measured on samples collected over one or two dimensional supports (Caniego et al. 2005; Zeleke and Si 2006; Zhang et al. 2013; Dafonte et al. 2015; Ji et al. 2016; Li et al. 2016). Until now, however, studies examining the spatial variability and singularity of soil nutrients and their scaling relationships using multifractal techniques still are more an exception than the rule.

Soil testing is the most common way of determining the nutritional status of plants, and therefore the base to evaluate fertilization rates. Soil testing involves extractions of available nutrients from the soil by a solution which is thought to mimic the root systems in terms of extracting nutrients from the soil. Currently, accredited laboratories of different countries, or even different states or provinces within a country, frequently utilize different soil test methods. Each specific protocol used to determine a selected nutrient is connected with a peculiar mechanism of extraction, and therefore different methods extract different pools of a nutritive element (Caridad Cancela et al. 2002; Vidal Vázquez et al. 2005).

Even if the spatial variability of soil and natural resources has been frequently addressed, very limited data are available on the effects of soil type and land use on soil nutrient extractability and on patterns of scaling heterogeneity of soil nutrient concentrations. Besides, calibration and comparison of soil testing methods is needed to accurately define how available nutrients are measured in soil samples. In general, comparison between extraction methods is merely based on Pearson correlation linear regression of results obtained by two soil testing methods, but the performance of this calibration was mostly below expectations (de Abreu et al. 1998; da Silva et al. 2015).

To our best understanding, until now no attempt has been made to compare concentrations of available soil nutrients measured by different methods at multiple scales. We hypothesized that the relationships between data on nutrient availability obtained by two different extraction methods may be scale dependent.

A sampling campaign was conducted to explore the spatial variability of P, K, Ca and Mg across small transects in soils representative of two contrasting agricultural areas of the autonomous community of Galicia, Spain. The aims of this work were: i) to characterize patterns of spatial variability of the studied available nutrients sampled along two short transects and determined with two different methods using the multifractal approach, and ii) to assess multiple scale relationships between the distributions of the concentrations of these available nutrients determined with two different methods using joint multifractals.

Material and Methods

Experimental fields and soil sampling

Soil samples were collected at two experimental fields (Figure 1). Field 1 is a vineyard located at the experimental site of "Viticulture and Enology Station of Galicia" (EVEGA) in Leiro, Ourense province, Spain (42º, 21′ 62′′ N, 8º 7′2′′W, and 110 m asl). At this site, mean annual temperature in the period 2000-2011 was 13.5 ºC and mean annual precipitation was 1247.82 mm. The soils at both sites are classified as Inceptisols (Umbrepts) in the US Soil Taxonomy (Soil Survey Staff, 2014). Field 2, devoted to polyculture (grassland intercropped with maize) is located at the experimental site of Mabegondo Agricultural Research Center (CIAM), A Coruña province, Spain, (43° 14' 47" N, Longitude 8° 16' 23" W, and 90 m asl). At this site, mean annual temperature in the period 2000-2011 was 13.9 ºC and mean annual precipitation was 1133.2 mm.

Field 1 is on a slight slope with a loamy sand textured soil (52.3% sand, 15.3% silt and 32.4% clay); mean soil pH is 4.9 and mean organic matter content 2.4%. Field 2 is on a moderate slope with a loamy textured soil (23.6% sand, 56.8% silt and 19.6% clay) mean soil pH is 5.3 and mean organic matter content 4.2%. In each field a 52 m transect was marked to collect soil samples, every 0.8 m, and therefore each transect consisted of 66 data points. Sampling was performed at 0 - 20 cm depth using a 5 cm diameter auger.

Analysis of macronutrients

Soil samples were air-dried, crushed and allowed to pass through a 2 mm sieve. Available P, K, Ca and Mg were extracted using both the Mehlich 3 solution (Mehlich, 1984) and an ion exchange resin (van Raij et al. 1986). Then, available P was determined by colorimetry (Paz-Ferreiro et al. 2012), while available K, Ca and Mg

were determined using inductively coupled plasma mass spectrometry (ICP-MS) (Caridad Cancela et al. 2002; Vidal-Vázquez et al. 2005).

Multifractal and joint multifractal analysis

To perform multifractal analysis firstly a measure should be defined, which is related to the local concentration of the studied variable across its geometrical support (Caniego et al. 2005; Vidal Vázquez et al. 2013). Here, concentrations of available P, K, Ca and Mg were converted into a distribution of mass along a one dimensional support.

Then a normalized probability mass function, $p_i(\delta)$, a variable, which describes the contribution of a segment (subinterval) of size δ to the total mass, was computed as:

$$p_i(\delta) = \varphi_i(\delta) / \sum_{i=1}^{n(\delta)} \varphi_i(\delta) \qquad (1)$$

Where φ_i is the value of the measure in the i^{th} segment at scale δ, $n(\delta)$ is the number of segments with size, δ, covering the sampling space, and $\sum_1^{N(\delta)} \varphi_i(\delta)$ represents the total mass of the whole transect.

In practice, two approaches are most commonly used for multifractal analysis of soil properties: the method of moments (Evertsz and Mandelbrot 1992) and the direct method (Chhabra and Jensen 1989). Here, generalized dimension spectra, D_q, and singularity spectra, $f(\alpha)$–α, were assessed by the former and the later method, respectively.

Using the moment method (Halsey et al. 1986), the so-called partition function $\chi(q,\delta)$, which results from a weighted sum of $p_i(\delta)$ over all the segments was defined as:

$$\chi(q,\delta) = \sum_{i=1}^{n(\delta)} [p_i(\delta)]^q \qquad (2)$$

Where statistical moments, q, are defined for $-\infty < q < \infty$. The partition functions when plotted against the segment or box size, δ, has the following scaling property:

148 $$\chi(q,\delta) \propto \delta^{-\tau(q)} \qquad (3)$$

149 Where, τ(q) is a non-linear function of *q*, which is known as the mass exponent
150 function.

151 In turn, the mass exponent function is related to the generalized fractal dimension
152 or Rényi dimension, Dq, (Hentschel and Procaccia 1983), which can be estimated as:

153 $$D_q = \frac{1}{q-1}\lim_{\delta\to 0}\frac{\log[\chi(q,\delta)]}{\log\delta} = \frac{\tau(q)}{q-1}, \text{ for } q \neq 1 \quad (4a)$$

154 Using Equation 4a, D_1 becomes indeterminate; thus, for the particular case that
155 q = 1, the following equation is used:

156 $$D_1 = \lim_{\delta\to 0}\frac{\sum_{i=1}^{n(\delta)} p_i(\delta)\log[p_i(\delta)]}{\log\delta}, \text{ for } q = 1 \qquad (4b)$$

157 The generalized dimensions, D_q for q = 0, q = 1 and q = 2, are known as the
158 capacity, the information (Shannon entropy) and correlation dimensions, respectively.
159 In homogeneous structures, D_q values are close to one another, whereas for a
160 monofractal structure they are equal.

161 Besides, multifractal distributed measures can be characterized by two other
162 scaling functions, which are defined as-implicit functions of q: the Hausdorf dimension,
163 $f(\alpha_q)$ and the average singularity strength, (α_q), as: $\tau(q) = q\ (\alpha_q) - f(\alpha_q)$. These scaling
164 functions can be estimated via Legendre transform, as: $f(\alpha_q) = q\ (\alpha_q) - \tau(q)$ and $\alpha_q =$
165 $d\tau(q)/dq$ (Evertsz and Mandelbrot 1992; Halsey et al. 1986).

166 Most commonly, however, f(α) and α are obtained using a direct method
167 (Chhabra and Jensen 1989). This procedure relies on the scaling properties of a
168 modified partition function, χ(q, δ), which is based on the contributions of individual
169 segment intervals. Thus, once the generating function has been obtained, the normalized
170 variable, $\mu_i(q,\delta)$, is defined by the following expression:

171 $$\mu_i(q,\delta) = \mu_i^{\,q}(\delta) / \sum_1^{n(\varepsilon)} \mu_i^{\,q}(\delta) \qquad (4c)$$

172 Then, using again a set of real numbers, $-\infty < q < \infty$, indices α and $f(\alpha)$ were computed
173 by the following relationships:

174 $$\alpha(q) \propto \frac{\sum_{i=1}^{N(\varepsilon)} \mu_i(q,\delta)\log[p_i(\delta)]}{\log(\delta)} \quad (5a) \quad \text{and} \quad f(\alpha(q)) \propto \frac{\sum_{i=1}^{N(\varepsilon)} \mu_i(q,\delta)\log[\mu_i(q,\delta)]}{\log(\delta)} \quad (5b)$$

175 A plot of $f(\alpha)$ versus α is called the multifractal or singularity spectrum, and
176 typically this plot has a parabolic concave downward shape, with the range of α values
177 increasing with the increase in the heterogeneity of the measure.

178 In our study, generalized dimension spectra, D_q, and singularity spectra, $f(\alpha)$-
179 α were calculated in the range of statistical moments $-5 \le q \le 5$ at 0.5 lag increments.

180 The joint partition function approach (Meneveau et al. 1990; Zeleke and Si 2006;
181 Ji et al 2016; Bertol et al. 2017) can be viewed as an extension of single multifractal
182 analysis, allowing joint characterization of the variability of two data sets along a
183 common transect. First, and based again in the box-counting idea, the total length of the
184 geometric support, which is common for all the pairs of variables studied, p and r
185 should be partitioned into boxes of size δ. The probability of the measures of these two
186 coexisting variables in the i^{th} segment are defined as $p_i(\delta)$ and $r_i(\delta)$. The local singularity
187 strength or Holder exponents of the two variables of interest, which are called α and β,
188 present the following relationship: $p_i(\delta) \propto (\delta)^{\alpha}$ and $r_i(\delta) \propto (\delta)^{\beta}$, respectively. Then,
189 similar to multifractal analysis of one variable, the normalized joint partition function,
190 $\mu_\iota(q,t,\delta)$, for the joint distribution of $p_i(\delta)$ and $r_i(\delta)$ was calculated as follows:

191 $$\mu_i(q,t,\delta) = \frac{[p_i(\delta)]^q\,[r_i(\delta)]^t}{\sum_{i=1}^{n(\varepsilon)}\,[p_i(\delta)]^q\,[r_i(\delta)]^t} \qquad (6)$$

192 Where q and t are real numbers representing the moment orders, and δ is the scale.

193 The singularity indices α(q,t) and β(q,t), were calculated as the average values of
194 α and β with respect to the μ measures defined by Equation6, based on the contributions
195 of individual segment intervals (Zeleke and Si 2006; Ji et al. 2016); these indices are
196 given, respectively by:

197 $$\alpha(q,t) = \lim_{\varepsilon \to 0} \frac{\sum_{i=1}^{n(\varepsilon)} \left[\mu_i(q,t,\delta) \cdot \log p_i(\delta)\right]}{\log \delta} \qquad (7a)$$

198 $$\beta(q,t) = \lim_{\varepsilon \to 0} \frac{\sum_{i=1}^{n(\varepsilon)} \left[\mu_i(q,t,\delta) \cdot \log r_i(\delta)\right]}{\log \delta} \qquad (7b)$$

199 The joint dimension f(α,β) of the set on which α(q,t) and β(q,t) are the mean local
200 singularity strengths of both measures is given by:

201 $$f(\alpha,\beta) = \lim_{\varepsilon \to 0} \frac{\sum_{i=1}^{n(\varepsilon)} \left[\mu_i(q,t,\varepsilon) \cdot \log \mu_i(q,t,\varepsilon)\right]}{\log \varepsilon} \qquad (8)$$

202 Joint multifractal spectra were obtained by plotting the joint dimension, f(α,β)
203 against singularity indices, α(q,t) and β(q,t). The joint distribution, f(α,β), for successive
204 pairs of values of the singularity indices α(q,t) and β(q,t), describes the distribution of
205 different intensity levels of one variable with respect to different intensity levels of the
206 other variable (Zeleke and Si 2006; Ji et al. 2016; Bertol et al. 2017). Note that for q = 0
207 or t = 0, the joint partition function (Eq. 6) becomes the partition function of a single
208 measure (Eq. 2). Therefore, similar to single multifractal analysis, if q = 0 and t = 0, the
209 maximum f(α,β) = f_{max} is attained.

210 ***Statistical analysis***

211 Descriptive statistical parameters (mean, median, maximum, minimum, standard
212 deviation, and coefficients of variation) were calculated to gauge data dispersion and
213 central tendency. Regression analysis was used to assess relationship between available
214 soil nutrients measured after extraction with exchange resin and Mehlich 3 at the single
215 scale and between scaling indices across the range of scales studied. The statistical

analysis was computed using SPSS Version 18.0 statistic software package(SPSS Inc., Chicago, Il., USA).

Results and Discussion

Single-scale analysis

Summary statistics of the available nutrient concentrations measured across the two transects are shown in Table 1. Mean values of the spatial distribution of available P, K, Ca and Mg were significantly higher ($p < 0.01$) under vineyard, than under polyculture and this irrespective of the extraction method. On average, levels of P, and K extracted with ion exchange resin were much lower than those extracted with Mehlich 3, at the two sites, and this was also the case for Ca and Mg under vineyard. However, under polyculture, levels of Ca and Mg extracted with ion exchange resin were higher than their counterparts extracted with Mehlich 3. These results suggest that the status of macronutrients depends on different soil properties and processes in the two areas studied.

The main difference between sites was on available levels of P and Mg. For example mean values of Mehlich 3 P were 246.79 mg kg^{-1} under vineyard and 39.27 mg kg^{-1} under polyculture. The high levels of available P under vineyard indicate overferlilization. Excess P text levels have been found in agricultural soils of the study region (Paz-Ferreiro et al. 2012) and subsequently risk of surface water eutrophication have been also reported (Sande Fouz et al. 2009; Mirás Avalos et al. 2012).

Spatial heterogeneity of the available nutrient concentrations at the measurement scale can be first characterized by coefficients of variation (CV). Statistical variability was higher under polyculture (CVs from 18.2% to 53.6%) compared to vineyard (7.5% to 19.0%). Coefficients of variation of available P and K were higher for resin than for Mehlich 3 extractions and this irrespective of the studied soil. The CV values of

available Ca and Mg also were higher for resin than for Mehlich 3 extractions under vineyard, but the reverse was true under polyculture in rotation.

Determination coefficients between the concentrations of available nutrients extracted with ion exchange membrane and Mehlich 3 solution showed significant positive correlations ($p < 0.01$) for the two transects studied (Table 3). The spatial distributions of resin and Mehlich 3 extracted P and K showed stronger correlations under vineyard. However, the spatial distributions of resin and Mehlich 3 extracted Ca and Mg showed much stronger correlations under polyculture.

Multifractal analysis

The distribution of a measure is considered fractal when the associated partition function for successive moments can be fitted by power law functions (Evertsz and Mandelbrot 1992). Therefore, firstly plots of the normalized measure $\chi(\theta, \delta)$ versus measurement scale, δ, were examined, for all the statistical moments of interest, to find out whether the spatial distributions of available nutrients obeyed or not power law scaling. Partition functions were calculated for moment orders in the range between $q = +5$ and $q = -5$, for successive box sizes in steps of L^{-k}, where L is the total segment length and k ranges from 0 to -6 (data not shown). For all the 16 spatial distributions of the available nutrients studied, and for statistical moments in the range $-5 < q < 5$, the logarithm of the normalized measures varied linearly with the logarithm of the measurements scale ($R^2 \approx 1.00$), and therefore demonstated power-law scaling.

The scaling properties observed can be further characterized to determine if there is a simple (monofractal) or multiple (multifractal) scaling types. Mono- and multifractal patterns of spatial distribution correspond to sources of variation of a different nature. While the former would be basically explained by a simple random fractal noise (close to a white noise) the latter arises from a much more complex

266 behaviour. Anyway, the multifractal property can be completely determined from the
267 entire spectra of the multifractal functions previously reported, i.e. mass exponent, τ_q,
268 generalized dimension, D_q, and singularity spectrum, $f(\alpha)$ versus α.

269 Generalized dimension spectra, D_q, computed at site 2, under polyculture are
270 shown in Figure 2. These are more or less typical sigma shaped curves with an inflexion
271 point at the point q = 0. However, D_q, spectra at site 1, under vineyard showed much
272 less curvature or even were quasi linear (data not shown). A sigma-shaped D_q is taken
273 as an indication of the multifractality of the measure, whereas a quasi-linear spectrum is
274 close to monofractals (Caniego et al. 2005; Zeleke and Si 2006; Roisin 2007; Vidal
275 Vázquez et al. 2013).

276 The value of D_1 is a good index of the degree of heterogeneity in the spatial
277 distribution of a measure (Zeleke and Si 2006; Vidal Vázquez et al. 2008; Paz-Ferreiro
278 et al. 2010) and it ranged from 1.00 to 0.97 (Table 2). The closer the D_1 value to D_0, the
279 more homogeneous is this distribution of the measure. Also width indices obtained from
280 the generalized dimension function, such as $w = (D_{-5} – D_5)$ showed wide differences,
281 ranging from 0.06 to 0.28 (Table 2). The higher the value of w index, the higher the
282 scaling heterogeneity of the spatial distribution of the available nutrients.

283 There were differences between sites regarding the shape of Dq curves, as well as
284 the values of multifractality parameters such D_1 and $w = (D_{-5} – D_5)$. For all the nutrients
285 studied and extractants employed, the entropy dimension, D_1, was equal or close to 1.00
286 under vineyard (1.00 to 0.99), but not under polyculture (0.99 to 0.97), also note that
287 using three decimal cases D_1 under vineyard becomes slightly smaller, as it ranges from
288 0.999 to 0.995 Similarly, amplitude, w, was lower at the former (0.01 to 0.04) than at
289 the latter (0.07 to 0.28). Therefore, a lower scaling heterogeneity of the soil nutrient
290 concentrations was found on the vineyard transect compared to that under polyculture in

291 rotation. Subsequently the former could be fitted reasonably well with multifractal
292 models, whereas the latter showed a trend to monofractal behaviour. Spatial distribution
293 exhibiting D_1 values very close to 1.00 have been described as quasi monofractal (Vidal
294 Vázquez et al. 2013). Thus, multifractal analysis allowed discriminations between
295 different patterns of spatial distribution of soil nutrients sampled across the studied
296 profiles.

297 Singularity spectra, $f(\alpha)$ versus α, were estimated by linear regression using
298 equations (5a) and (5b), for the range of moments $-5 < q < 5$, while taking a $R^2 = 0.90$
299 value as a threshold, so that pairs of values $f(\alpha)$ versus α below this threshold were not
300 accepted. Using this rule, $f(\alpha)$-α plots were obtained for positive q moment orders
301 varying from 4.5 to 5, and for negative q moment orders ranging from -3.5 to -5 (data
302 not shown). As expected, widths of the singularity spectra, (α_{max}-α_{min}), and those of the
303 generalized dimension spectra, ($D_{-5} - D_5$), showed a similar rank for all the spatial
304 distributions studied. Thus, for the spatial distributions of P, K, Ca and Mg under
305 polyculture, the multifractal behaviour is very clearly expressed in the shape and
306 parameters of the singularity spectrum, and this is consistent with the analysis of the
307 generalized dimension spectra. Again, the spatial distributions of these nutrients under
308 vineyard showed a scarce amplitude of the D_q and $f(\alpha)$-α spectra, which correspond to
309 quasi monofractal behaviour.

310 The spatial variability of selected soil nutrients characterized by single
311 multifractal spectrum was not completely consistent with the result of CV analysis. This
312 is an expected result, as multifractal spectra were obtained over a wider range of spatial
313 scales and moment orders, while CVs, only reflect the spatial variability at the
314 measurement scale.

315 Quantification of soil spatial variability is a prerequisite to predict soil properties
316 at unsampled locations, and to upscaling/downscaling patterns of spatial variability. In
317 this study, the spatial variability of selected soil nutrients characterized by multifractal
318 parameters would have practical significance for prediction and for transferring
319 information of these available nutrients from one scale to another. Appropriate
320 prediction procedures for variables with high spatial variability and a large amount of
321 singularity indices are different than those for variables with low spatial variability and
322 narrow singularity indices (Caniego et al. 2005; Zeleke and Si 2006; Zhang et al. 2013;
323 Li et al. 2016; Ji et al. 2016). The scaling properties of the spatial distributions of the
324 soil nutrients studied, mainly suggested a monofractal scaling behaviour under
325 vineyard. However, under polyculture in rotation, the spatial distributions showed a
326 tendency to be multifractal. When the spatial distribution of a variable is the response of
327 some linear processes, it shows monofractal behaviour and the scaling can be done
328 using a single coefficient over multiple scales. However, when the spatial distribution is
329 the nonlinear response of multiple factors and processes acting over a variety of scales,
330 multiple scaling indices are required for quantifying the spatial variability (Zeleke and
331 Si 2006; Vidal Vázquez et al. 2013; Ji et al. 2016).
332 The vineyard is characterized by higher concentrations of available P, K, Ca and
333 Mg, than the polyculture area, meaning that agricultural management practices in the
334 latter lead to higher nutrient inputs. However, the area devoted to polyculture exhibits a
335 higher spatial variability and spots with the largest or the smallest concentrations of
336 available elements. For example available Ca shows higher maximum and lower
337 minimum values under compared to vineyard.
338 Therefore, differences in the multifractality of the available nutrient for the two
339 soils studied are the results of differences in the soil forming factors and processes and

in agricultural management practices within these two areas. Subsequently, not only different procedures are needed for upscaling/downscaling information about the spatial distribution of soil nutrients, but also differing fertilization strategies will be required in the two areas for optimal land management.

Joint multifractal analysis

Results of the joint distributions obtained for the two studied sites, are shown in Figures 3 and 4, respectively. These plots highlight the joint dimensions, f(α,ß) of two variables coexisting across a common support, whose singularity indices α(q,t) and β(q,t) are represented in the horizontal and the vertical axis, respectively. The x-axis in contour plots displayed at Figures 3 and 4 corresponds to nutrients extracted with Mehlich 3 , while the respective y-axis corresponds to those extracted with resin. Table 3 compares coefficients of determinations (R^2) between concentrations of nutrients determined by the two soil tests methods, at the single scale (i.e. the observation or measurement scale), and those of the respective scaling dimensions, α(q,t) and β(q,t) at various spatial scales, obtained by joint multifractal analysis.

Joint multifractal spectra are commonly represented by contour lines portraying the scaling relationship of the distribution of high or low values of a given variable with respect to the distribution of high or low values of its counterpart. The bottom left part of the contours shows the joint dimension of the high values of the two variables, and the top right part show that of the low data values. Therefore, the scaling indices of two variables are positively correlated if the resulting joint spectrum of the distribution, f(α,ß), presents high values of α(q,t) and β(q,t) at the top right part and low values of α(q,t) and β(q,t) at the bottom left part. Conversely, low values of α(q,t) and β(q,t) at the bottom right part, and high values of α(q,t) and β(q,t) at the top left part of the f(α,ß) spectrum indicates a strong correlation between high values of one variable and low

values of the other one. Moreover, the lower the stretch of the diagonal contours at the f(α,ß) spectrum, the stronger the correlation between the scaling indices of pair of variables of interest (Zeleke and Si 2006; Zhang et al. 2013; Bertol et al. 2017).

Table 3 shows that under vineyard, the strongest positive correlations were obtained between the scaling indices α(q,t) and β(q,t), for the joint distributions of Mehlich 3 P versus resin P (R^2 = 0.92) and Mehlich 3 K versus resin K (R^2 = 0.96). Similarly, under polyculture in rotation, the strongest positive correlations were obtained between the scaling indices α(q,t) and β(q,t), for the joint distributions of Mehlich 3 K versus resin K (R^2 = 0.97) and Mehlich 3 Ca versus resin Ca (R^2 = 0.99). This is also evident as the respective contour plots are diagonally oriented and rather pooled together (Figures 3 and 4). In general coefficients of determination at multiple scales, i.e. those obtained by regression between scaling indices of the joint distributions Mehlich 3 versus resin, were $R^2 > 0.63$. Strong association between nutrients extracted by Mehlich 3 and ion exchange membrane point out that the relationships between the spatial distributions obtained by these two extraction methods are valid across all spatial scales. Thus, the heterogeneity in the spatial distributions obtained when using one of soil test is well-reflected in the heterogeneity obtained when its counterpart is utilized, and viceversa.

Joint multifractal analysis of available nutrients extracted by ion exchange resin and Mehlich 3 corroborates different degrees of association between the respective scaling indices, α(q,t) and β(q,t). In joint multifractal analysis, the stronger the correlation at multiple scales the more similar is expected to be the ensemble of factors and processes driven their intermittency. Conversely, when an intermittent and a smooth variable coexist along a common spatial support, a weak joint exponent is expected,

389 suggesting that factors and processes driven the variability of two coexisting variables
390 are different (Zeleke and Si 2006; Bertol et al. 2017).

391 Pearson correlations obtained from regression between available nutrients
392 extracted by resin and Mehlich 3 at the observation scale were, in general, weaker than
393 those between the scaling indices $\alpha(q,t)$ and $\beta(q,t)$. For all the data sets studied,
394 correlations at the single scale ranged from $R^2 = 0.54$ to $R^2 = 0.95$, while at the multiple
395 scale they ranged from $R^2 = 0.63$ to $R^2 = 0.97$. For joint multifractals there may be a
396 strong joint exponent $f(\alpha)$ if two variables are highly correlated at multiple scales, even
397 if Pearson correlation at the observation scale may be weak.

398 Many studies have been devoted to compare concentrations of available nutrients
399 extracted by different methods and to calibrate these methods, but until now they
400 merely considered a single scale, and therefore they used linear correlation between
401 pairs of data values, which may not be valid at other scales. Across the short transects in
402 this study, factors and processes impacting the availability of soil nutrients are expected
403 to be much more complicated and heterogeneous than that of the simple point sampling
404 commonly used in calibration of soil test methods. Also, the major controlling processes
405 for availability of different soil nutrients may differ at different landscapes and soil uses,
406 which would further impact the spatial variability of soil nutrients. The results of joint
407 multifractal analysis in this study had demonstrated the ability of this approach to
408 provide new insight when soil test methods are compared and calibrated, because of his
409 performance in characterizing the scaling relationships between selected soil nutrients
410 across a transect.

411

412

413

Conclusions

This work presents two case studies focusing on the spatial distribution of available soil nutrients extracted by two different methods. Concentrations of available P, K, Ca and Mg showed higher mean values and lower statistical variability (lower CVs) on a vineyard than under polyculture in rotation.

The spatial distributions of soil nutrient concentrations under polyculture in rotation could be fitted reasonably well with multifractal models, while those on the vineyard showed a trend to monofractal behaviour and could be described as quasi multifractal. Therefore transferring information about spatial variability from one scale to another requires multiple scaling indexes on the former land use and a single scaling index on the latter land use.

Joint multifractal analysis corroborates different degrees of association between the respective scaling indices. It also showed that in general available nutrients were stronger correlated at multiple scales than at the observation scale. Therefore, single scale analysis may not be sufficient to fully describe relationships between soil testing methods.

References

Armstrong AC. 1986. On the fractal dimensions of some transient soil properties. J Soil Sci. 37(4):641-652.

Baveye P, Laba M. 2015 Moving away from the geostatistical lamppost: Why, where, and how does the spatial heterogeneity of soils matter? Ecol Modell. 298: 24-38.

Bertol I, Schick J, Bandeira DH, Paz-Ferreiro J, Vidal Vázquez E. 2017. Multifractal and joint multifractal analysis of water and soil losses from erosion plots: A case study under subtropical conditions in Santa Catarina highlands, Brazil. Geoderma 287:116-125.

Caniego FJ, Espejo R, Martín MA, San José F. 2005. Multifractal scaling of soil spatial variability. Ecol Modell.182:291-302.

Caridad-Cancela R, de Abreu CA, Paz-González A. 2002. DTPA and Mehlich3 extractability in natural soils. Commun Soil Sci Plant Anal.33 (15-18):2879-2893.

Caridad-Cancela R, Vidal Vázquez E, Vieira SR, Abreu CA, Paz González A. 2005. Assessing the spatial uncertainty of mapping trace elements in cultivated fields. Commun Soil Sci Plant Anal. 36, (1-3):253-274.

Chhabra AB, Jensen RV. 1989. Direct determination of the f(α) singularity spectrum. Phys Rev Lett. 62:1327-1330.

Dafonte Dafonte J, Valcarcel Armesto M, da Silva Dias R, Vidal Vázquez E, Paz-González A. 2015. Assessment of the spatial variability of soil chemical properties along a transect using multifractal analysis. Cadernos Lab Xeolóxico de Laxe. 38:11-24.

462 da Silva Dias R, de Abreu CA, de Abreu MF, Paz González A. 2015. Statistical
463 Methods for Evaluating Results from Soil Micronutrient Analyses in Interlaboratory
464 Programs. Commun Soil Sci Plant Anal. 46:57-71.
465 de Abreu CA, de Abreu MF, de Andrade JC, van Raij B. 1998. Restrictions in
466 the use of correlation coefficients in comparing methods for the determination of the
467 micronutrients in soils. Commun Soil Sci Plant Anal. 29(11-14):1961-1972.
468 Everstz CJG, Mandelbrot, BB. 1992. Multifractal measures. In Peitgen, H.,
469 Jürgens, H., and Saupe, D. Chaos and Fractals. Berlin(BE): Springer. p. 921-953.
470 Grout H, Tarquis AM, Wiesner MR. 1998. Multifractal analysis of particle size
471 distributions in soil. Environ Sci Technol. 32 (9):1176-1182.
472 Halsey TC, Jensen MH, Kanadoff LP, Procaccia I, Shariman BI. 1986. Fractal
473 measures and their singularities: the characterization of strange sets. Phy. Rev A. .
474 33:1141-1151.
475 Hentschel HGE, Procaccia I. 1983. The infinite number of generalized
476 dimensions of fractals and strange attractors. Physica D. 8:435-444.
477 Ji W, Lin M, Biswas A, Si BC, Chau HW, Cresswell HP. 2016. Fractal
478 behavior of soil water storage at multiple depths. Nonlinear Process Geophys.
479 23:269-284.
480 Li X, Li X, Yuang F, Jowitt S, Zhou T, Yang K, Zou J, Li Y. 2016. Comparison
481 of the multifractal characteristics of heavy metals in soils within two areas of
482 contrasting economic activities in China. Nonlinear Process Geophys. 23(5):331-339.
483 Mc Bratney AB, Webster R. 1986. Choosing functions for semi-variograms of
484 soil properties and fitting them to sampling estimates. J Soil Sci.37:617-639.
485 Mehlich A. 1984. Mehlich 3 soil test extractant: A modification of Mehlich 2
486 extractant. Commun Soil Sci Plant Anal. 15(12):1409-1416.

Meneveau C, Sreenivasan KR, Kailasnat P, Fan MS. 1990. Joint multifractal measures. Theory and applications to turbulence. Phys Rev A. . 41:894-913.

Miranda JGV, Montero E, Alves MC, Paz-González A, Vidal Vázquez E. 2006. Multifractal characterization of saprolite particle-size distributions after topsoil removal. Geoderma. 134:373-385.

Mirás Avalos JM, Sande Fouz P, Bertol I, Paz González A. 2012. Crop residue effects on Ca, Mg, K and Na runoff losses from a soil prone to crusting. Commun Soil Sci Plant Anal. 43:315-323.

Morales LA, Vidal Vázquez E, Paz-Ferreiro J. 2011. Influence of liming on the spatial and temporal variability of Mehlich-1 extractable Fe in a rice field. J Geochem Explor. 109 (1-3):78-85.

Paz-Ferreiro J, Miranda JGV, Vidal Vázquez E, 2010. Multifractal analysis of soil porosity based on mercury injection and nitrogen adsorption. Vadose Zone J. 9:325-335.

Paz-Ferreiro J, Vidal Vázquez E, de Abreu CA. 2012. Phosphorus determination after Mehlich-3 extraction and anion exchange resin in an agricultural soil of Northwestern Spain. Commun Soil Sci Plant Anal. 43 (1-2):102-111.

Perfect E, Kay BD. 1995. Applications of fractals in soil and tillage research: A review. Soil Till Res. 36:1–20

Roisin CJ. 2007. A multifractal approach for assessing the structural state of tilled soils. Soil Sci Soc Am. J. 71:15-25.

Sande Fouz F, Mirás Avalos JM, Vidal Vazquez E, Paz González A. 2009. Phosphorus contents and loads at the outlet of an agroforestry catchment in northwestern Spain. Commun Soil Sci Plant Anal. 40 (1-6): 660-671.

Soil Survey Staff. 2014. Keys to Soil Taxonomy, 12th Edition, Natural Resources Conservation Service, Washington DC, 360 pp.

SPSS Inc. Released 2009. PASW Statistics for Windows, Version 18.0. Chicago: SPSS Inc.

van Raij B, Quaggio JA, da Silva NM. 1986. Extraction of phosphorus, potassium, calcium, and magnesium from soils by an ion exchange resin procedure. Commun Soil Sci Plant Anal. 17, 5:547-566.

Vidal Vázquez E, Caridad-Cancela R, Taboada-Castro MM, Paz-González A, de Abreu CA. 2005. Trace elements extracted by DTPA and Mehlich-3 from agricultural soils with and without compost additions. Commun Soil Sci Plant Anal. 36 (4-6):712-727.

Vidal Vázquez E, Miranda JGV, Alves MC, Paz González A. 2006. Effect of tillage on fractal indices describing soil surface microrelief of a Brazilian Alfisol. Geoderma. 134 (3-4):428-439

Vidal Vázquez E, Paz-Ferreiro J, Miranda JGV, Paz González A. 2008. Multifractal analysis of pore size distributions as affected by simulated rainfall. Vadose Zone J. 7(2):500-511.

Vidal Vázquez E, Camargo OA, Vieira SR, Miranda JGV, Menk JRF, Siqueira GM, Mirás-Avalos JM, Paz González A. 2013. Multifractal analysis of soil properties along two perpendicular transects. Vadose Zone J.12 (3):13pp.

Zeleke TB, Si BC, 2006. Characterizing scale-dependent spatial relationships between soil properties using multifractal techniques. Geoderma. 134:440-452.

Zhang F, Yin G, Wang Z, McLaughlin N, Geng X, Liu Z. 2013. Quantifying Spatial Variability of Selected Soil Trace Elements and Their Scaling Relationships Using Multifractal Techniques. Plos One. 8 (7).

Tables

Table 1. Descriptive statistics of the concentrations of available P, K, Ca and Mg extracted in mg kg^{-1}. (Std = standard deviation; CV = coefficient of variation; subindex 'res' means extraction with exchange resin, while subindex Mh-3 means extraction with the Mehlich 3 solution).

	Mean	Median	Std	Minimum	Maximum	C.V.
EVEGA, Leiro (Site 1)						
P_{res}	70.18	67.00	13.37	47.00	101.00	19.04
P_{Mh-3}	246.94	242.91	42.00	182.62	357.27	17.01
K_{res}	298.77	308.87	52.56	168.12	390.98	17.59
K_{Mh-3}	508.99	514.53	58.96	373.27	624.05	11.58
Ca_{res}	585.78	581.16	82.99	400.80	801.60	14.17
Ca_{Mh-3}	803.17	797.63	62.36	651.83	948.73	7.76
Mg_{res}	139.10	133.68	17.46	109.37	182.29	12.55
Mg_{Mh-3}	288.52	291.92	21.68	242.72	344.89	7.52
CIAM, Mabegondo (Site 2)						
P_{res}	12.45	10.00	6.26	6.00	39.00	50.25
P_{Mh-3}	39.27	36.59	10.93	25.75	83.39	27.83
K_{res}	138.98	136.85	28.00	89.93	218.96	20.15
K_{Mh-3}	229.90	233.47	41.74	144.66	337.62	18.16
Ca_{res}	508.57	480.94	154.69	300.59	1001.95	30.42
Ca_{Mh-3}	471.03	448.11	161.23	216.03	960.21	34.23
Mg_{res}	38.99	33.43	16.88	15.80	83.88	43.30
Mg_{Mh-3}	33.68	27.57	18.05	1.84	80.48	53.60

Table 2. Generalized dimension values for selected q moment orders (D_{-5}, D_5, D_1 and D_2) and width of e spectra, $w = (D_{-5}, D_5)$.

Nutrient	D_5	D_{-5}	D_1	D_2	D_{-5}-D_5
EVEGA Leiro (Site 1)					
P_{res}	0.98 ± 0.00	1.02 ± 0.00	0.99 ± 0.00	0.99 ± 0.00	0.04
P_{Mh-3}	0.98 ± 0.00	1.02 ± 0.00	1.00 ± 0.00	0.99 ± 0.00	0.04
K_{res}	0.99 ± 0.00	1.02 ± 0.00	1.00 ± 0.00	0.99 ± 0.00	0.03
K_{Mh-3}	0.99 ± 0.00	1.01 ± 0.00	1.00 ± 0.00	1.00 ± 0.00	0.02
Ca_{res}	0.99 ± 0.00	1.01 ± 0.00	1.00 ± 0.00	0.99 ± 0.00	0.02
Ca_{Mh-3}	1.00 ± 0.00	1.00 ± 0.00	1.00 ± 0.00	1.00 ± 0.00	0.00
Mg_{res}	0.99 ± 0.00	1.01 ± 0.00	1.00 ± 0.00	1.00 ± 0.00	0.02
Mg_{Mh-3}	1.00 ± 0.00	1.00 ± 0.00	1.00 ± 0.00	1.00 ± 0.00	0.00
CIAM Mabegondo (Site 2)					
P_{res}	0.87 ± 0.00	1.06 ± 0.01	0.98 ± 0.00	0.96 ± 0.01	0.19
P_{Mh-3}	0.93 ± 0.01	1.03 ± 0.00	0.99 ± 0.00	0.98 ± 0.00	0.10
K_{res}	0.95 ± 0.01	1.02 ± 0.00	0.99 ± 0.00	0.98 ± 0.00	0.07
K_{Mh-3}	0.96 ± 0.01	1.02 ± 0.00	0.99 ± 0.00	0.99 ± 0.00	0.06
Ca_{res}	0.96 ± 0.00	1.04 ± 0.00	0.99 ± 0.00	0.98 ± 0.00	0.08
Ca_{Mh-3}	0.94 ± 0.00	1.05 ± 0.01	0.99 ± 0.00	0.98 ± 0.00	0.11
Mg_{res}	0.92 ± 0.02	1.06 ± 0.02	0.98 ± 0.00	0.96 ± 0.01	0.14
Mg_{Mh-3}	0.90 ± 0.02	1.18 ± 0.02	0.97 ± 0.01	0.94 ± 0.01	0.28

Table 3. Coefficients of determination (R^2) between the concentration of P, K, Ca and Mg extracted by exchange resin and Mehlich 3 solutions (single or measurement scale) and between the respective scaling indices $\alpha(q,t)$ and $\beta(q,t)$ at multiple spatial scales.

	EVEGA, Leiro (Site 1)		CIAM, Mabegondo (Site 2)	
	Single scale	Scaling indices	Single scale	Scaling indices
P	0.82	0.92	0.80	0.89
K	0.87	0.96	0.79	0.97
Ca	0.62	0.87	0.95	0.99
Mg	0.54	0.63	0.93	0.92

553 **Figure captions**

554 **Figure 1.** Location of the two studied fields. CIAM Mabegondo (Site 2),
555 extraction with Mehlich 3 solutionCIAM Mabegondo (Site 2), extraction with
556 exchange resin

557

558 **Figure 2.** Generalized dimension spectra of available P, K, Ca and Mg
559 extracted by ion exchange resin and Mehlich 3 solution at site 2 under polyculture in
560 rotation.

561

562 **Figure 3.** Multifractal spectra of the joint distribution of P, K, Ca and Mg
563 extracted using Mehlich 3 solution (horizontal axis) and ion exchange resin (vertical
564 axis) at EVEGA Leiro, on a vineyard. (Different grey intensities show the joint
565 dimension of the two scaling indices: $\alpha(q,t)$ and $\beta(q,t)$.)

566

567 **Figure 4.** Multifractal spectra of the joint distribution of P, K, Ca and Mg
568 extracted using Mehlich 3 solution (horizontal axis) and ion exchange resin (vertical
569 axis) at CIAM Mabegondo, under polyculture in rotation. (Different grey intensities
570 show the joint dimension of the two scaling indices: $\alpha(q,t)$ and $\beta(q,t)$.

571

572

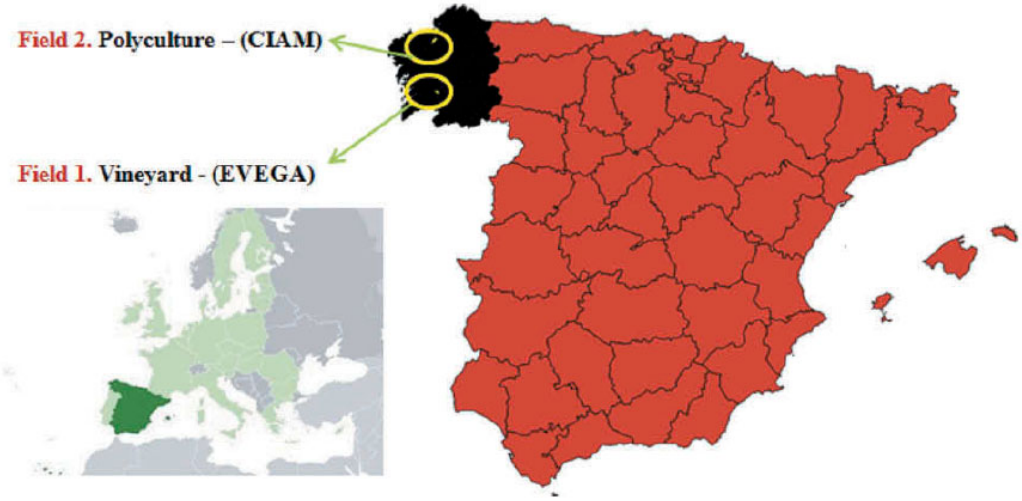

573

574 **Figure 1.**

575

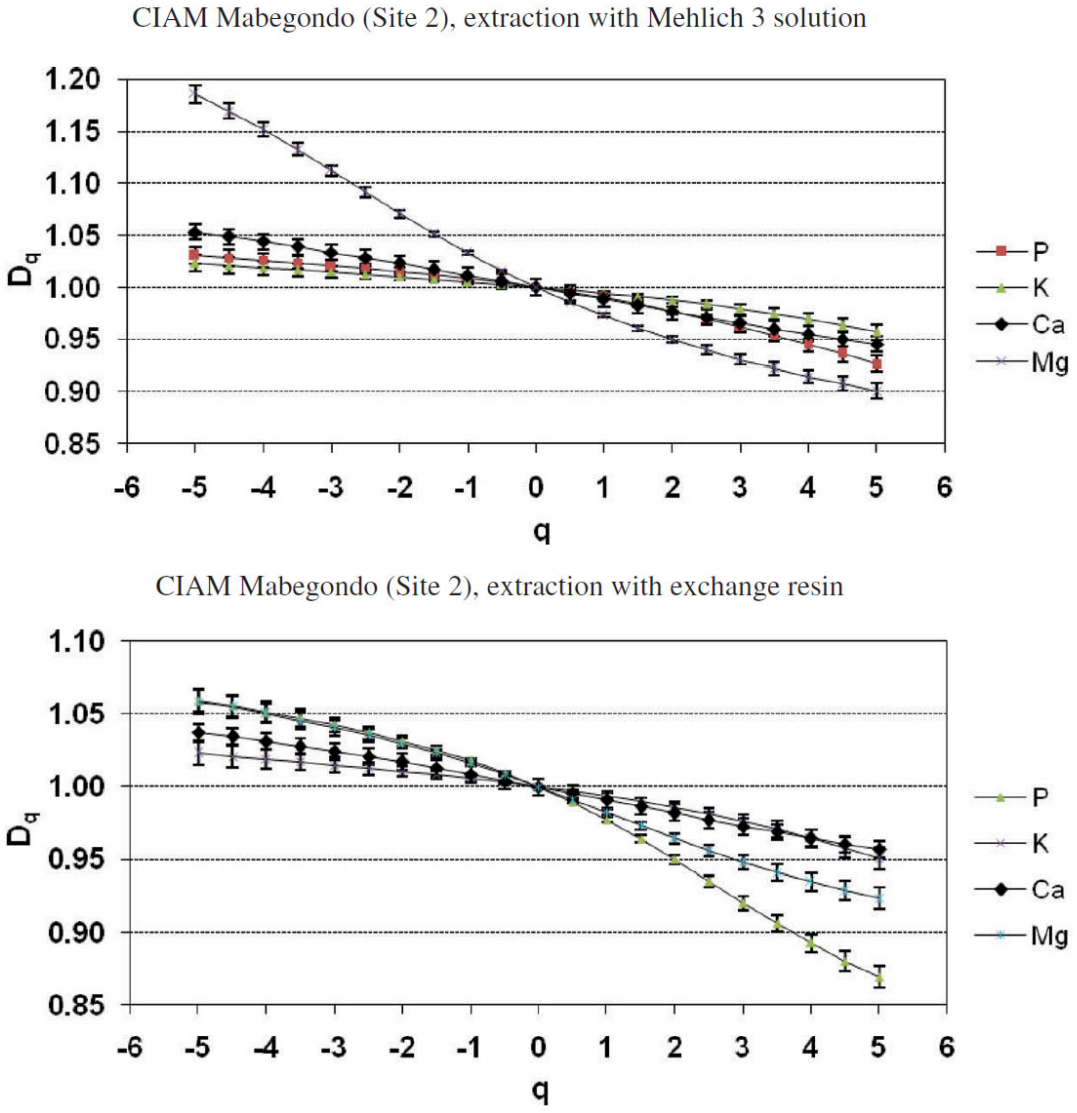

576

577 **Figure 2.**

578

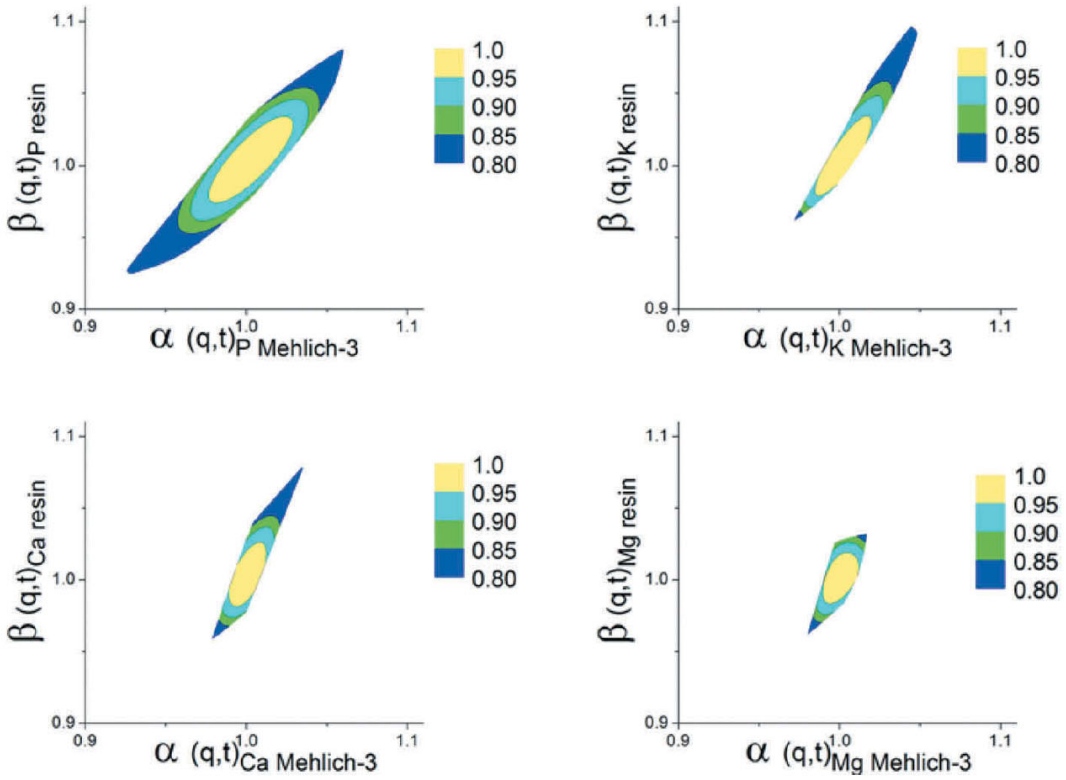

579

580 **Figure 3.**

581

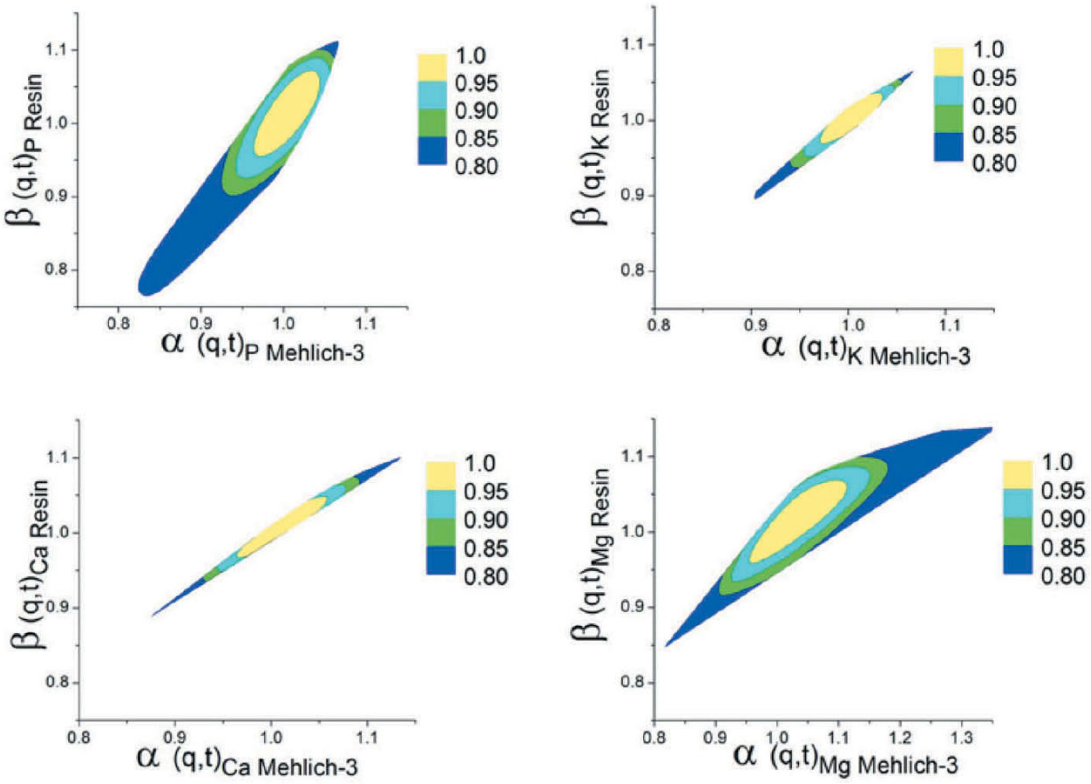

582

583 **Figure 4.**

584